Generation of Lipid Polarity in Intestinal Epithelial (Caco-2) Cells: Sphingolipid Synthesis in the Golgi Complex and Sorting before Vesicular Traffic to the Plasma Membrane

Wouter van 't Hof and Gerrit van Meer

Department of Cell Biology, Medical School, University of Utrecht, 3584CX Utrecht, The Netherlands

Abstract. Generation of intestinal epithelial lipid polarity was studied in Caco-2 cells. Confluent monolayers on filters incorporated the exchangeable lipid *N*-6-NBD-aminocaproyl-sphingosine (C6-NBD-ceramide) from liposomes. The fluorescent ceramide was converted equally to C6-NBD-glucosylceramide and C6-NBD-sphingomyelin, analogues of lipids enriched on the apical and basolateral surface, respectively, of intestinal cells in vivo. Below 16°C, where vesicular traffic is essentially blocked, each fluorescent product accumulated in the Golgi area. At 37°C, 50% had been transported to the cell surface within 0.5 h, as measured by selective extraction of the fluorescent lipids onto BSA in the medium ("back-exchange") at 10°C. Transport to the two surfaces could be assayed separately, as a diffusion barrier existed for both NBD-lipids and BSA. C6-NBD-glucosylceramide was enriched twofold apically, whereas C6-NBD-sphingomyelin was equally distributed over both domains. Polarities did not decrease when 37°C incubations were carried out in the presence of increasing BSA concentrations to trap the fluorescent lipids immediately after their arrival at the cell surface. Within 10 min from the start of synthesis, both products displayed their typical surface polarity. Lipid transcytosis displayed a half time of hours. In conclusion, newly synthesized sphingolipids in Caco-2 cells are sorted before reaching the cell surface. Transcytosis is not required for generating the in vivo lipid polarity.

ENTEROCYTES express a strictly polarized function in the selective absorption of digested dietary products from the small intestinal lumen and transepithelial transport into the internal milieu of the body. This is reflected by a division of the cell surface into two domains by the tight junction, the zonula occludens, which circles the apex of each enterocyte and seals the cell monolayer into an effective barrier. While the apical surface domain lines the intestinal lumen and is covered with extended microvilli, the brush border, the basolateral plasma membrane faces neighboring cells, the basal lamina, and underlying tissue. To meet their different physiological demands, the two membranes possess unique protein and lipid compositions. Digestive hydrolases are typically apical constituents. Furthermore, the apical surface is exceptional in that it is covered by glycosphingolipids. In contrast, most plasma membrane proteins expressed by both epithelial and nonepithelial cells, such as MHC class I antigens and Na^+-K^+ ATPase, are located in the basolateral domain, which is also enriched in the common phospholipids sphingomyelin (SPH)[1] and phosphatidylcholine. Lipid polarity, a typical two- to fivefold unilateral enrichment, is less absolute than that of the proteins (41, 43, 45).

The generation of protein and lipid polarity involves the segregation of apical and basolateral plasma membrane constituents after biosynthesis at a common site. In the kidney-derived MDCK cells, apical and basal components are sorted at the exit of the Golgi complex, whereupon they are directly transported to their respective destinations via vesicular transport pathways. Transcytosis, the Golgi-independent transcellular vesicle pathway, in MDCK cells possesses apical/basolateral sorting potential as well, but is not essential for biosynthetic sorting (5, 32). In hepatocytes a direct vesicular pathway from the Golgi complex to the apical surface seems nonexistent. Apical membrane proteins are shuttled basolaterally first. Sorting from basolateral proteins apparently occurs during subsequent transcytosis (22). In intestinal cells, some in vivo studies have provided evidence for the involvement of both the direct and indirect route in the biosynthetic transport of apical membrane proteins (18, 35, 39), whereas others found no significant contribution of an indirect transcytotic route (1, 7, 13, 16, 33).

The introduction of in vitro systems has been of great value to the field (22, 37). For example, the human intestinal cell line Caco-2 spontaneously differentiates into monolayers of highly polarized cells with a characteristic brush border and an appropriate transepithelial electrical resistance (15, 20, 38). Caco-2 cells originate from a colonic adenocarcinoma, but resemble small intestinal enterocytes. They secrete lipo-

1. *Abbreviations used in this paper*: GlcCer, glucosylceramide; SPH, sphingomyelin.

proteins and a plasma lipid transfer protein into the basal medium (10, 11). In addition, they express brush border hydrolases (19), a most interesting property considering the confusing in vivo data on the routing of these proteins to the apical domain.

A direct pathway from the Golgi to the apical surface exists in Caco-2 (9, 36; and in other colonic cells, reference 29). However, the basal secretion of over 90% of native secretory proteins, of a lysosomal protein during inhibition of lysosomal targeting, and of secretory proteins transfected into Caco-2 as tracers for bulk flow constitutive secretion, has led to the suggestion that perhaps also 90% of the membrane protein transport goes to the basolateral surface (23, 40). The direct apical pathway was also judged to be only modestly developed from the finding that three newly synthesized apical proteins were inserted simultaneously into both surfaces, with subsequent sorting and rearrangement of the basolateral fraction to the apical membrane by transcytosis, while a basolateral protein appeared in the basolateral membrane only (36). All in all, protein sorting at the exit of the Golgi complex seems less absolute than in MDCK. Therefore, in intestinal cells also transcytosis is required for targeting newly synthesized apical membrane proteins. The predominant hypothesis is that the incomplete sorting at the level of the Golgi is due to a reduced size of the direct apical pathway.

In MDCK cells, plasma membrane lipids are sorted after synthesis in ER and the Golgi complex before the carrier vesicles leave the Golgi complex (48), just like membrane proteins. Here, we have characterized sorting of newly synthesized lipids in Caco-2 and asked whether it is different from that in MDCK. The fluorescent lipids C6-NBD-glucosylceramide (GlcCer) and C6-NBD-SPH were biosynthetically accumulated in the Golgi complex, after which delivery to the two cell surfaces was quantitated by selective depletion of the probes onto a scavenger (BSA) in the medium. The fluorescent lipids are analogues of the major native glycosphingolipid GlcCer and of SPH, which are enriched two- to threefold on the apical (GlcCer) and the basolateral (SPH) cell surface of enterocytes (25). In Caco-2 cells, like in MDCK, newly synthesized sphingolipids were sorted before reaching the cell surface. In contrast to its role in targeting of apical membrane proteins, transcytosis did not significantly contribute to biosynthetic lipid sorting. Finally, no indications were found for a reduction in the size of the direct apical transport pathway in Caco-2.

Materials and Methods

Cell Culture

Caco-2 cells (38) of high passage (160–175) were subcultured weekly and grown in a hydrated atmosphere (5% CO_2 in air) in 75-cm^2 flasks using DME (4.5 g/l glucose), supplemented with 20% FCS (heat-inactivated), 1% nonessential amino acids, 100 U/ml penicillin and 100 μg/ml streptomycin. Cells were passaged using trypsin-EDTA at a surface dilution of 1:25 (19). For experiments, cells were grown on 0.45-μm pore-size transparent microporous collagen-treated membranes of 24.5-mm-diam (Transwell-COL, Costar, Cambridge, MA). Filter inserts were suspended in six 20-mm-high polypropylene rings, and placed into a 150-mm-diam glass dish with 100 ml medium. 4 h after plating, medium in the filter inserts was replaced to remove loose cells. Apical medium was changed every second day, starting 3 d after plating. Cell density was monitored by transmission light microscopy. Confluence was also assayed by the reduction in the transepithelial passage of ^{125}I-BSA. By both assays Caco-2 cells plated at a density of 4.8×10^4 cells/4.7 cm^2-filter reached confluence after 5 d. Experiments were performed after 7 d, when each filter contained about 2.5×10^6 cells and had a typical transepithelial resistance of 170 $\Omega \cdot cm^2$. This increased to 850 $\Omega \cdot cm^2$ after 14 d with 4.5×10^6 Caco-2 cells/filter.

Incubation Conditions

Incorporation of C6-NBD-Lipids. Monolayers on filters were taken from the incubator, washed twice with Hanks' balanced salt solution (HBSS) and placed in a 6-well cluster dish containing 2.0 ml of HBSS per well at 10°C. C6-NBD-ceramide (19.5 nmol in 750 μl, 13 mol percent in unilamellar phosphatidylcholine liposomes; reference 48) was applied to the apical surface for 0.5 h. After removal of the liposomes and two washes with HBSS, unless indicated otherwise, cells were incubated for 2 h at 20°C. Under these conditions, the lipid partitions into the cellular membranes and reaches the site where it is metabolically converted to C6-NBD-GlcCer and C6-NBD-SPH (48). The hydrophilicity of the C6-NBD-chain is responsible for rapid equilibration of this class of molecules between membranes across the aqueous phase, while the absence of the polar head group on the ceramide allows it to flip across membranes (26, 30, 31, 48). Lipid transport to the cell surface was studied at 37°C after cultures had received fresh HBSS.

C6-NBD-Lipid Transport. Transport of C6-NBD-GlcCer and C6-NBD-SPH to each of the two cell surfaces was assayed by "back-exchange" (30). The principle of the assay is a selective depletion of the C6-NBD-lipids from the cell surface by, in this case, 1% BSA (wt/vol) in HBSS (HBSS+BSA). Apparently by virtue of its hydrophobic binding sites, BSA efficiently extracts C6-NBD-GlcCer and C6-NBD-SPH from the plasma membrane surface (48). In some experiments, the presence of the NBD-lipids on the cell surface was monitored by performing a back-exchange after the 37°C transport incubation. To this end, the 37°C-medium was replaced by 10°C-HBSS+BSA for two times 0.5 h. In other experiments, the delivery of the NBD-lipids to the cell surface was monitored continuously by having BSA present in the HBSS during the transport incubation. At the end of the incubation, the filter was transferred to a cluster dish on an ice-cold metal plate, and the medium was replaced by fresh HBSS+BSA for two times 0.5 h at 10°C to wash any fluorescent lipid-containing BSA out of the filter and to ensure complete back-exchange. After each incubation, apical and basal HBSS were collected and their fluorescent lipids analyzed. While 85% of the apical NBD-lipids was typically extracted into the 37°C-HBSS+BSA and 15% into the two subsequent 10°C-HBSS+BSA media, these values were 75% and 25%, respectively, for the basolateral NBD-lipids. After the last incubation, the filter was cut from its holder for analysis of cellular lipids.

Lipid Analysis

Lipids from cells and media were extracted according to Bligh and Dyer (3). All aqueous solutions were acidified to 10 mM acetic acid. Separation, identification by two-dimensional high-performance thin layer chromatography and quantitation of fluorescent lipids were performed as described (48). Metabolic products were identified as C6-NBD-GlcCer and C6-NBD-SPH by comparison to authentic standards. Filters with attached cells were extracted in 1 ml of the one-phase mixture. The filter was removed before separation of the mixture into two phases. Fluorescent spots were scraped from the plates and extracted from the silica in 2 ml of $H_2O/CH_3OH/CHCl_3$ (1:2.2:1; vol/vol) for 0.5 h. After pelleting the silica for 10 min at 1,500 g_{max}, fluorescence (λ_{ex} = 470 nm; λ_{em} = 535 nm) in the supernatant was quantified using a SFM fluorimeter (Kontron Elektronik GmbH, Zürich, Switzerland). When nonfluorescent extracts were analyzed, the resulting GlcCer or SPH spot gave a background value equivalent to 0.9 $\pm$ 0.2 (n = 15) pmol C6-NBD-SPH. Within any experiment two background values were always within 0.1 pmol.

Calculation of Polarity and Sorting

Polarity. The polarity of each NBD-lipid is defined as the apical/basolateral ratio; i.e., the amount of the lipid found in the apical over that in the basal HBSS+BSA after an incubation at 37°C- and then 10°C, C6-NBD-$GlcCer_{ap}$/C6-NBD-$GlcCer_{bl}$ and C6-NBD-SPH_{ap}/C6-NBD-SPH_{bl}.

Sorting. As a measure of sorting of C6-NBD-GlcCer from C6-NBD-SPH, the polarity of C6-NBD-GlcCer was compared to that of C6-NBD-SPH. The quotient of these ratios is termed the relative $polarity_{GlcCer/SPH}$. It represents the enrichment of C6-NBD-GlcCer over C6-NBD-SPH in the apical plasma membrane domain as compared to the basolateral domain.

$$\text{Relative Polarity}_{\text{GlcCer/SPH}} = \frac{\dfrac{\text{C6-NBD-GlcCer}_{ap}}{\text{C6-NBD-GlcCer}_{bl}}}{\dfrac{\text{C6-NBD-SPH}_{ap}}{\text{C6-NBD-SPH}_{bl}}} = \frac{\dfrac{\text{C6-NBD-GlcCer}_{ap}}{\text{C6-NBD-SPH}_{ap}}}{\dfrac{\text{C6-NBD-GlcCer}_{bl}}{\text{C6-NBD-SPH}_{bl}}}$$

Microscopy

Cell monolayers on the transparent filters were viewed on an inverted light microscope. Confocal laser scanning microscopy was performed on an MRC-500 instrument (Bio-Rad Lasersharp, Ltd., Abingdon, UK) mounted onto a Zeiss Axioplan microscope. For electron microscopy Caco-2 cells on Transwell-COL's were fixed in 0.5% glutaraldehyde and 2.5% formaldehyde in 0.1 M sodium cacodylate buffer (pH 7.2) for 1 h at 4°C. The filters were cut from their holders, postfixed in 2% OsO_4, dehydrated through a series of ethanol solutions, and embedded in Epon. Thin sections were stained with uranyl acetate and lead citrate, and examined in a JEOL 1200EX transmission electron microscope (Tokyo, Japan).

Materials

C6-NBD-analogues of ceramide, GlcCer and SPH were synthesized as before (48). Culture media and solutions were obtained from Gibco Laboratories (Glasgow, UK), FCS from Boehringer Mannheim GmbH (Mannheim, FRG), and culture plastics were from Costar (Cambridge, MA). BSA, fraction V, was purchased from Sigma Chemical Co. (St. Louis, MO). Chemicals and solvents were of analytical grade and obtained from E. Merck (Darmstadt, FRG).

Results

Site of Synthesis of C6-NBD-GlcCer and C6-NBD-SPH in Caco-2 Cells on Transwell-COL Filters

Confluent monolayers of Caco-2 cells were grown on collagen-coated filters. In addition to more closely mimicking physiological conditions, this configuration permitted accessibility to the basolateral cell surface that was essential for lipid transport studies. The Caco-2 cells were highly polarized. Already at 2 d after confluence, they had differentiated into columnar cells with a well-developed apical brush border, characteristic of small intestinal epithelial cells (Fig. 1, *a* and *b*).

As a first step in studying the generation of lipid polarity, the site of sphingolipid biosynthesis was characterized. For this, C6-NBD-ceramide was presented to Caco-2 cells and the cells kept below 20°C (48). After 4 h at 15°C, over 50% of the ceramide had been converted to C6-NBD-GlcCer and C6-NBD-SPH (Table I). By this time, fluorescence had accumulated in discrete perinuclear structures (Fig. 2 *a*) that in various cell types have been identified as the Golgi complex (see Discussion). To specifically localize each metabolic product, the experiment was repeated in the presence of the C6-NBD-lipid acceptor BSA. At the end of the incubation most of the C6-NBD-ceramide was found in the medium, whereas 80–90% of the C6-NBD-GlcCer and C6-NBD-SPH was resistant to back-exchange by BSA and remained cell-associated (Table I). Therefore, the bulk of the products must have been synthesized intracellularly; BSA, present throughout the incubation, should have removed any fluorescent product reaching the cell surface. Essentially, all cellular fluorescence remaining in the presence of BSA was Golgi area located (Fig. 2 *b*). This must apply for both C6-NBD-GlcCer and C6-NBD-SPH, as in this experiment they accounted for 41% and 26% of the intracellular fluorescence, respectively (Table I).

Transport of the C6-NBD-Lipids to each Cell Surface Can Be Assayed Separately

When C6-NBD-GlcCer and C6-NBD-SPH were accumulated in the Golgi area at 15°C and the cells subsequently warmed to 37°C, the plasma membrane became labeled at the expense of the Golgi fluorescence (Fig. 2, *a* and *c*); NBD-lipids were transported to the cell surface. To study appearance at each plasma membrane domain separately, NBD-lipids on the one surface should not be accessible to BSA added to the opposite side. To test this, Caco-2 monolayers were allowed to synthesize C6-NBD-GlcCer and C6-NBD-SPH for 2 h at 20°C (where conversion was more efficient than at 15°C), after which the cells were warmed to 37°C to chase a substantial fraction to the cell surface (cf., Fig. 2 *c*). Leakage of NBD-lipids between the two membrane domains was subsequently tested at 10°C, where vesicular traffic but not lateral diffusion should be blocked (Table II). For this, BSA was selectively added to either the apical (*II*) or the basolateral surface (*III*). In controls, BSA was added to both surfaces (*I*). First of all, cellular NBD-lipids were not depleted into the media without BSA, indicating that BSA was required for NBD-lipid depletion and also that under test conditions, substantial BSA leakage across the cell monolayer did not occur. In addition, essentially all C6-NBD-GlcCer and C6-NBD-SPH that should be present on the surface incubated without BSA, according to the control (*I*), was resistant to extraction by BSA present on the opposite side of the monolayer. It was indeed recovered from the correct surface in the subsequent BSA-incubation.

Polarity of Delivery and Sorting of C6-NBD-GlcCer and C6-NBD-SPH

After 1 h at 37°C about equal fractions of C6-NBD-GlcCer and C6-NBD-SPH, over 55%, were present on the cell surface (Table II). However, the apical/basolateral polarity was very different for the two lipids: 1.7 for C6-NBD-GlcCer versus 0.8 for C6-NBD-SPH. C6-NBD-GlcCer had a relative polarity of 2.1 as compared to C6-NBD-SPH. Thus, during the combined processes after accumulation in the Golgi complex, including Golgi-plasma membrane transport, endocytosis and possibly transcytosis, the lipids had been sorted.

To find out whether endocytosis (and transcytosis) were involved in lipid transport to the apical surface (see Introduction) and in the generation of lipid polarity, BSA was included in the 37°C-media to trap C6-NBD-GlcCer and C6-NBD-SPH immediately after their arrival at the cell surface. As a first result, more NBD-lipids were trapped by 1% and 2% BSA than was found on the cell surface after 1 h in the absence of BSA (Fig. 3 *a*). The reduction in the fraction at the cell surface in the absence of BSA was not due to incomplete back-exchange, as a third BSA-incubation at 10°C did not release NBD-lipids over background values. It must have been caused by reinternalization of NBD-lipids after their arrival at the cell surface.

In the presence of BSA the apical/basolateral polarity of delivery at 37°C was somewhat higher for both lipids (Fig. 3 *b*; Table III). No further increase was observed between

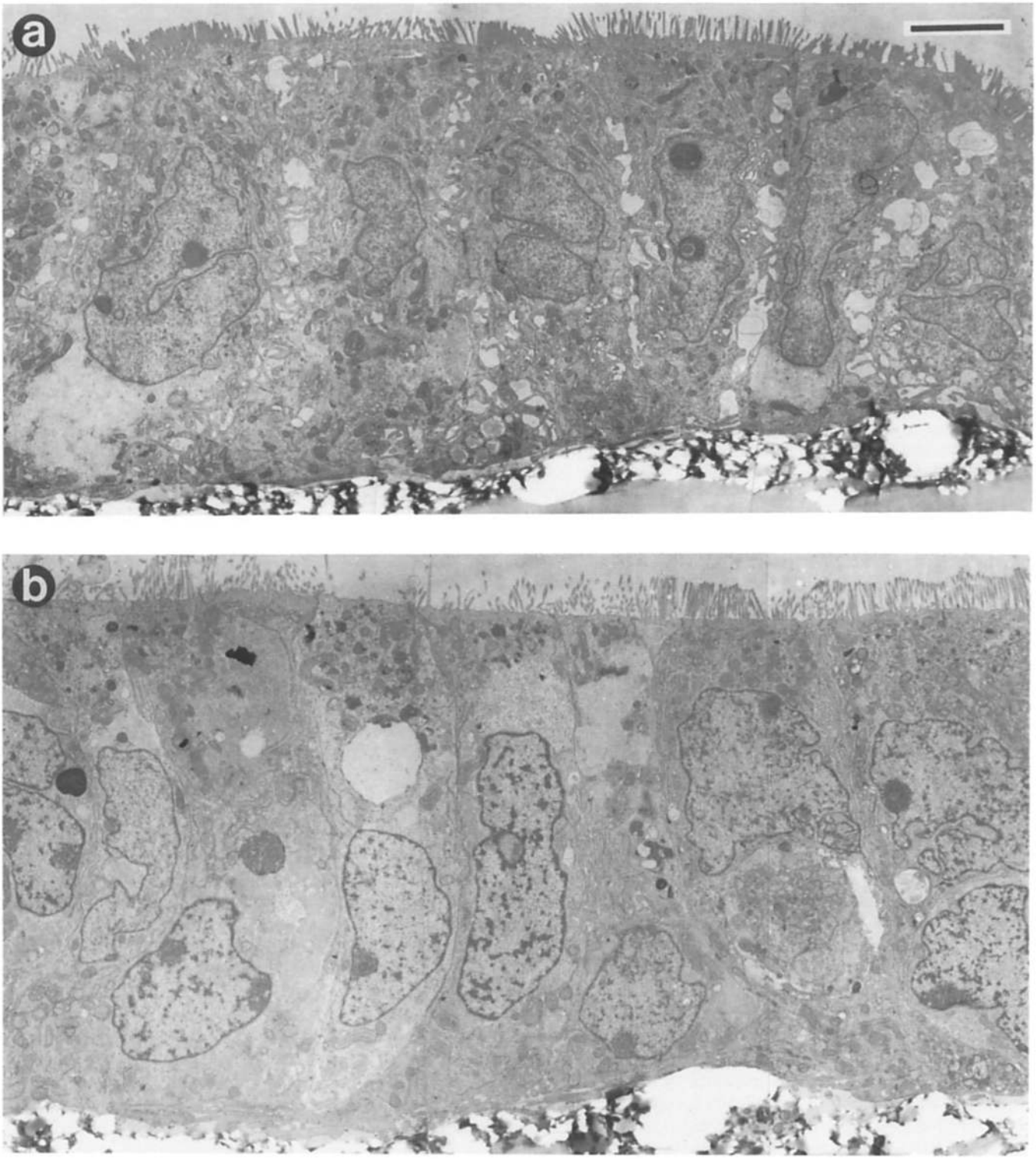

Figure 1. Electron micrographs of Caco-2 cells on Transwell-COL filters (Costar). (*a*) 7 d after plating, and (*b*) 14 d after plating. With age, the height of the cells increases from 19 to 23 μm, the length of the microvilli nearly doubles from 0.9 to 1.6 μm, lateral spaces become condensed, and the nuclei turn heterochromatic. Growth on traditional Millipore filters (Millipore Continental Water Systems, Bedford, MA) has been reported (9). However, BSA did not penetrate these filters well enough to allow efficient back-exchange (48). The transparent microporous collagen-treated Transwell-COL membranes were found to be a good alternative. Bar, 4 μm.

1% and 2% BSA, arguing that at 1% essentially all C6-NBD-GlcCer and C6-NBD-SPH appearing at the surface was trapped. Therefore, under these conditions only direct transport from the Golgi to each plasma membrane was monitored. Since relative polarity, a measure of lipid sorting (see Materials and Methods), was not reduced in the presence of BSA (Fig. 3 *c*; Table III), sorting between the two lipids must have occurred before they reached the cell surface.

Table I. Intracellular Synthesis of C6-NBD-GlcCer and C6-NBD-SPH (pmol/10^6 cells)

Location of NBD-lipids after 4 h at 15°C	C6-NBD-ceramide	C6-NBD-GlcCer	C6-NBD-SPH
Cells	35.5 ± 0.5	27.6 ± 0.6	19.0 ± 1.0
HBSS	5.7 ± 0.2	0.3 ± 0.0	0.3 ± 0.0
Cells	15.3 ± 1.0 (33%)*	18.7 ± 1.2 (41%)	12.1 ± 0.6 (26%)
HBSS + 2% BSA	52.7 ± 0.5	2.3 ± 0.2	3.1 ± 0.5

Cell monolayers on filters were incubated with C6-NBD-ceramide for 0.5 h at 10°C. After three washes, HBSS or HBSS + 2% BSA (wt/vol) was added to the cells, and the incubation continued for 4 h at 15°C. Subsequently, cells and combined apical and basolateral incubation media were analyzed. Two filters were averaged for each point. Total synthesis (per 10^6 cells) in the presence of BSA was 21 pmol C6-NBD-GlcCer 89% of which was intracellular and 15 pmol of C6-NBD-SPH, 80% intracellular. After 4 h at 10°C, synthesis was 7 pmol C6-NBD-GlcCer, 84% intracellular, and 9 pmol C6-NBD-SPH, 86% intracellular (n = 6). After 4 h at 0°C, corresponding values were 3 pmol C6-NBD-GlcCer, 86% intracellular, and 6 pmol C6-NBD-SPH, 92% intracellular (n = 4).
* Parenthetical numbers represent the percentage of cellular fluorescence.

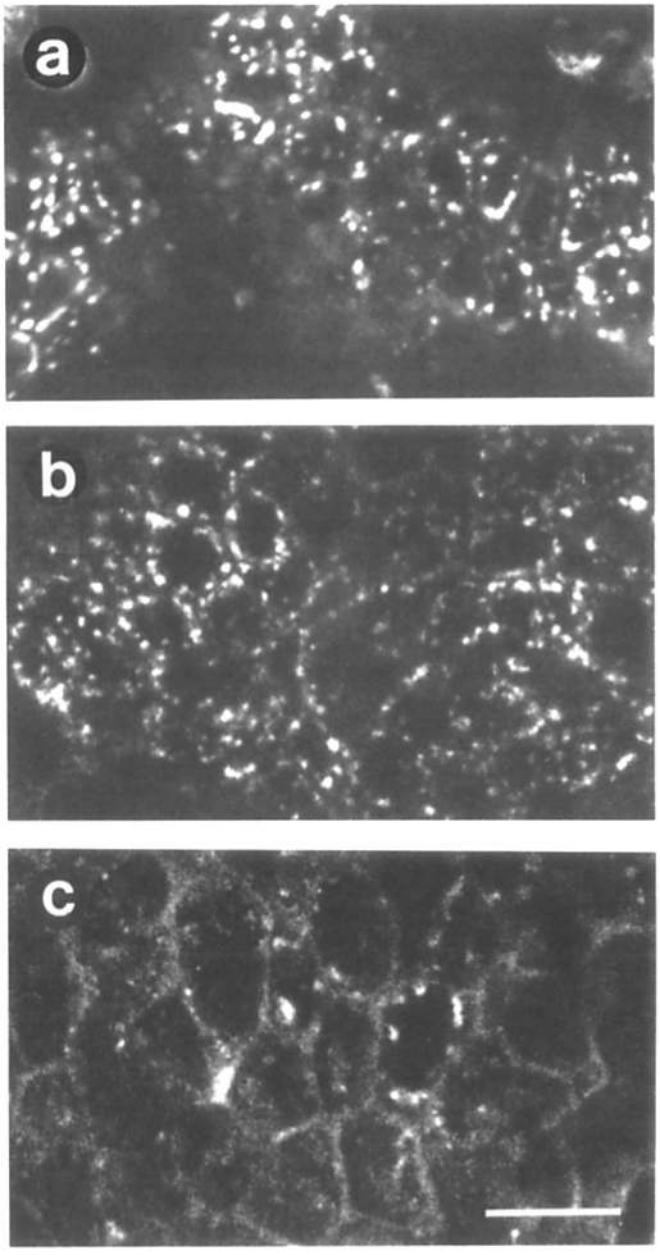

Figure 2. Metabolic accumulation of C6-NBD-GlcCer and C6-NBD-SPH in the Golgi area at low temperature. After the addition of C6-NBD-ceramide and subsequent washes, Caco-2 cells were incubated for 4 h at 15°C in the absence (*a* and *c*) or presence (*b*) of 2% BSA. BSA depletes fluorescent lipids from the cell surface and C6-NBD-ceramide from all over the cell (Table I). In *c*, the 4-h incubation was followed by 1 h at 37°C in the absence of BSA. The initial Golgi pattern of the fluorescence changed into staining of the plasma membrane and peripheral cytoplasm. Images were obtained by confocal scanning laser microscopy. Thickness of optical sections is ± 1 μm. Bar, 20 μm.

Kinetics of Lipid Transport to the Apical and the Basolateral Surface

As an independent approach to the question of how C6-NBD-GlcCer and C6-NBD-SPH reach the apical plasma membrane domain, the kinetics of appearance in the apical and basolateral media were determined (Figs. 4 and 5). If apical NBD-lipids would pass over the basolateral membrane (see Introduction) and, for some reason, escape depletion by basolateral BSA, this would show up as a lag in the appearance in the apical medium and in lower initial apical/basolateral polarities.

In a first approach, the two lipids were accumulated in the Golgi complex at 20°C before the transport measurement at 37°C. The preincubation was carried out in HBSS+BSA, and was followed by 0.5 h at 10°C in HBSS+BSA. Both served to clear the surface of any NBD-lipids that might reside there, due to either synthesis at the surface or transport at 20°C, and that would interfere with subsequent 37°C transport measurements, particularly on short time scales. In Fig. 4, no lag in apical arrival is observed. Already within the first 10 min at 37°C fractions of both NBD-lipids were recovered in the apical medium. In addition, the polarities within the first 10 min for both lipids were very similar to those measured after longer time intervals (cf., Table III).

To exclude the possibility that the delivery measured within the first 10 min at 37°C was partially a consequence of transport processes that had been initiated during the preceding 20°C incubation, the experiment was repeated without preincubation. Under these conditions C6-NBD-GlcCer and C6-NBD-SPH had not been synthesized and accumulated in the Golgi area before the 37°C transport assay. Synthesis and transport started at the same time, immediately after removal of the C6-NBD-ceramide containing liposomes and warming of the cells to 37°C. The results were very similar to those of the previous experiment (Fig. 5). The NBD-lipids were delivered to both cell surface domains within 5–10 min from the start of the 37°C incubation, and polarities within those first minutes were similar to those found after longer time intervals. According to these data,

Table II. C6-NBD-GlcCer and C6-NBD-SPH on One Surface Are Not Depleted by BSA Present in the Medium on the Opposite Side at 10°C

Compartment	C6-NBD-GlcCer (pmol/10^6 cells)		C6-NBD-SPH (pmol/10^6 cells)	
	Incubation 1 (0.5 h)	Incubation 2 (2 × 0.5 h)	Incubation 1 (0.5 h)	Incubation 2 (2 × 0.5 h)
I Cells	–	11.0	–	13.2
Apical HBSS	–	8.9	–	8.2
Basal HBSS	–	5.2	–	9.9
II Cells	–	10.2	–	13.7
Apical HBSS	7.9	2.1	6.5	2.0
Basal HBSS	(−BSA) 0.8	4.3	(−BSA) 0.1	8.3
III Cells	–	11.7	–	13.9
Apical HBSS	(−BSA) 1.0	7.8	(−BSA) 1.0	6.3
Basal HBSS	3.7	2.2	7.1	4.5

Cell monolayers were incubated with C6-NBD-ceramide, washed, and left for 2 h at 20°C (Materials and Methods). Transport of the fluorescent lipids to the cell surface was allowed to proceed for 1 h at 37°C in the absence of BSA. Subsequently, the cells were incubated selectively at 10°C in the presence of BSA on the apical (*II*) or the basal side (*III*). (*Incubation 1*, the absence of BSA is indicated by [−BSA].) After 0.5 h, HBSS+BSA was added to both sides for 0.5 h at 10°C, which was repeated once, to analyze the fraction of the two NBD-lipids left on each cell surface (*Incubation 2*). Control filters were incubated twice with HBSS+BSA on both sides for 0.5 h (*I*). The media of the last two incubations were pooled, and cells and media were analyzed. Deviations from the mean (two filters per condition) were ≤10% (average, 6%) for the values over 4 pmol, and 17% (average) for smaller values. Of the total fluorescence <2% was recovered in the 37°C medium without BSA (n = 12).

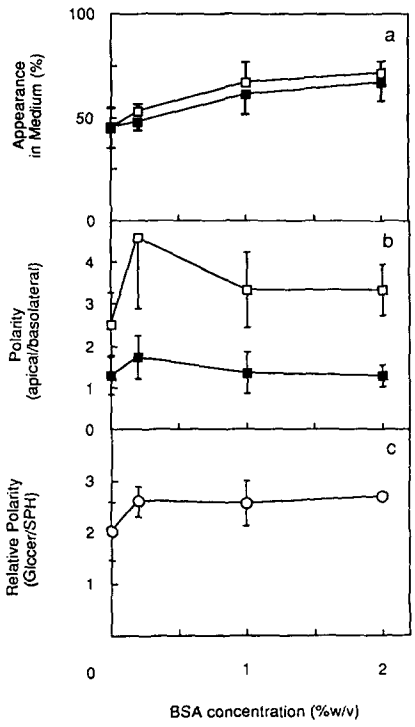

Figure 3. Immediate depletion of C6-NBD-ClcCer and C6-NBD-SPH by BSA during the 37°C incubation does not affect the polarity of their delivery. Caco-2 monolayers were incubated with C6-NBD-ceramide, followed by 2 h at 20°C, and 1 h at 37°C in HBSS with concentrations of BSA as indicated on the abscissa. After two subsequent 0.5-h incubations at 10°C with BSA to complete the back-exchange, the cells, the combined apical incubation media, and the combined basal media were analyzed for C6-NBD-GlcCer (□) and C6-NBD-SPH (■). (*a*) *Appearance in medium*, expressed as sum of the deliveries to the two surfaces. (*b*) *Apical/basolateral ratio*, polarity of delivery. (*c*) *Relative polarity*$_{GlcCer/SPH}$, sorting. In each experiment, at least two BSA concentrations were compared: 0% BSA, n = 6; 0.2%, n = 3; 1%, n = 8; 2%, n = 3.

transcytosis was either not involved in apical transport or its half time was <5 min.

Lipid Transcytosis

A first approximation of the rate of transcytosis of NBD-lipids was obtained by a simple variation on the lipid transport assay. Instead of having BSA in the 37°C media on both sides (Table IV, *I*), BSA was selectively omitted from the medium on one side of the cell monolayer (Table IV, *II* and *III*). Since the NBD-lipids were depleted from the surface with BSA, but not from the surface without BSA, only the latter remained available for endocytosis and transcytosis during the 37°C incubation. Transcytosis should now appear as an increased delivery to the cell surface that was exposed to the BSA, as compared to parallel monolayers where BSA was present on both surfaces. The latter (Table IV, *I*) served to measure direct transport from the Golgi complex to each plasma membrane domain.

Of the NBD-lipids that had been delivered to a plasma membrane domain as measured in the control (Table IV, *I*), only 70% was still present on that surface after 1 h at 37°C in the unilateral absence of BSA (Table IV, *II* and *III*). Of the 30% lost, 22% was found intracellularly. The increase in intracellular fluorescence was 0.7 ± 0.2 of the loss from the surface incubated without BSA (n = 28). It proved additive when BSA was omitted from both sides (Table IV, *IV*). Most of the endocytosed NBD-lipids were present in a recycling compartment, as in an independent experiment 71 ± 12% (n = 5) reappeared at the cell surface during a subsequent 37°C incubation for 1 h in the presence of BSA.

When BSA was left out of the basal or apical medium (Table IV, *II* and *III*), 8% of the 30% fluorescence lost from the surface without BSA was recovered from the medium on the opposite side after 1 h at 37°C, a possible indication for transcytosis. However, a similar effect was observed in the leakage experiment at 10°C at which temperature transcyto-

Table III. Sorting and Polarized Delivery of C6-NBD-GlcCer and C6-NBD-SPH to the Plasma Membrane at 37°C, after Intracellular Accumulation at 20°C

Age of cells (d)	BSA	Polarity (C6-NBD-GlcCer) (apical/basolateral)	Polarity (C6-NBD-SPH) (apical/basolateral)	Relative polarity (sorting)
7	0%	2.2 ± 0.7	1.1 ± 0.4	2.1 ± 0.4 (n = 12)
7	1%	3.4 ± 0.6	1.3 ± 0.3	2.7 ± 0.4 (n = 30)
14	1%	3.6 ± 0.5	0.5 ± 0.1	6.7 ± 0.2 (n = 2)

Cell monolayers were incubated with C6-NBD-ceramide, followed by 2 h at 20°C and 1 h at 37°C in the presence of 0% or 1% BSA, as in Fig. 3. Subsequently, the cells were incubated twice in HBSS+BSA for 0.5 h at 10°C. Combined apical media and combined basal media were analyzed for NBD-lipids and the apical/basolateral ratio was determined. Relative polarity was calculated for each individual measurement. Transport to the cell surface: after 20, 37, and 10°C in 7 d, 0% BSA, 42 ± 7% of the C6-NBD-GlcCer and 43 ± 5% of C6-NBD-SPH were recovered from the medium. For 7 d, 1% BSA, this was 73 ± 10% and 69 ± 9%, and for 14 d, 1% BSA, transport was 65 ± 2% and 62 ± 1%, respectively. The ratio of newly synthesized C6-NBD-GlcCer over C6-NBD-SPH after 20, 37, and 10°C was 0.8 ± 0.1 in 11 independent experiments.

sis should be inhibited (Table II), suggesting the involvement of some other mechanism. Consequently, no direct evidence was found for transcytosis of NBD-sphingolipids within 1 h at 37°C. The results of this indirect assay indicate that the half time of lipid transcytosis must be hours, while 50% of the newly synthesized lipids had reached the cell surface by the direct pathway from the Golgi complex within 30 min (Figs. 4 and 5). Because of the low level of transcytosis and high standard deviations, it was not possible to determine whether transcytosis was higher in the one or other direction and whether it was different for the two NBD-lipids. For this purpose, a more direct assay is now being developed.

Discussion

The present paper characterizes the cell surface delivery of two newly synthesized fluorescent lipids to elucidate the sorting event responsible for the segregation of apical from basolateral lipids in Caco-2 cells. Lipid sorting is compared to that in MDCK cells, where the sorting of plasma membrane proteins seems different from that in Caco-2.

Site of Synthesis of C6-NBD-SPH and C6-NBD-GlcCer and Mechanism of Transport

The newest evidence clearly shows that SPH biosynthesis is essentially confined to the Golgi complex. The enzyme has now been localized to the *cis*- and *medial*-Golgi complex by subfractionation of rat liver, with <13% of the activity present at the plasma membrane (14, 24). Evidence for a luminal orientation of SPH-synthase was provided by controlled protease digestion of intact and permeabilized Golgi vesicles

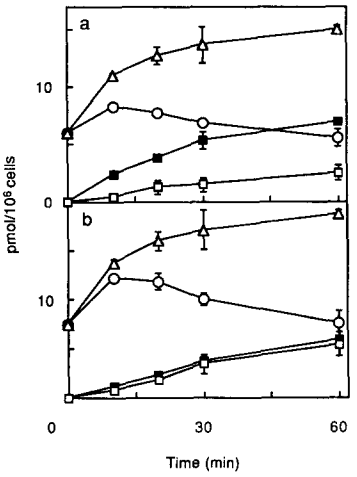

Figure 4. Appearance of C6-NBD-GlcCer (*a*) and C6-NBD-SPH (*b*) in the medium on either side of a Caco-2 monolayer at 37°C, after accumulation in the Golgi complex at 20°C. Cells were incubated with C6-NBD-ceramide followed by 2 h 20°C in HBSS + BSA (Materials and Methods). The cell surface was subsequently cleared of any remaining NBD-lipids (0.5 h at 10°C with BSA). At t = 0, fresh apical and basal HBSS+BSA was added to a series of parallel monolayers at 37°C. After defined time intervals, the medium was collected and replaced by 10°C-HBSS+BSA for 0.5 h (twice) to complete the back-exchange. Cells (○) and the combined 37°C- and final 10°C-media from the apical (■) and from the basal side (□) were analyzed; (△) sum. Data points are the mean of four independent experiments with duplicate measurements. Error bars, SD.

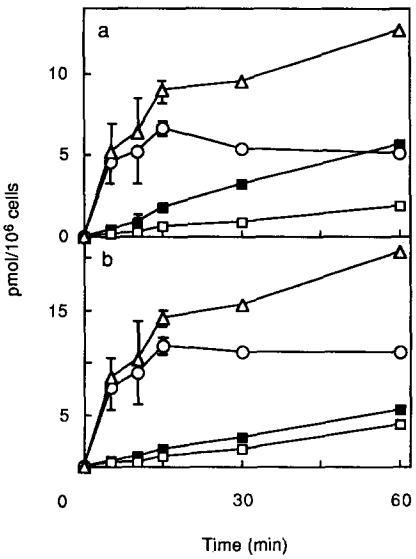

Figure 5. Appearance of C6-NBD-GlcCer (*a*) and C6-NBD-SPH (*b*) in the medium on either side of a Caco-2 monolayer at 37°C, without 20°C preincubation. Cells were incubated with C6-NBD-ceramide containing liposomes at 10°C, and washed. At t = 0, fresh HBSS+BSA of 37°C was added to both sides of the monolayer. After defined time intervals, the medium of a filter was collected and replaced by fresh HBSS+BSA of 10°C for 0.5 h (twice) to complete the depletion. Analyses and symbols as in Fig. 4.

Table IV. Transcytosis of Newly Synthesized C6-NBD-Sphingolipids during 1 h at 37°C

Compartment	37°C	C6-NBD-GlcCer Percentage of total	C6-NBD-GlcCer (Test/Control)	C6-NBD-SPH Percentage of total	C6-NBD-SPH (Test/Control)
		%		%	
I Cells		34	–	40	–
Apical HBSS		50	–	31	–
Basal HBSS		16	–	29	–
II Cells		36	(1.12 ± 0.17)*	46	(1.20 ± 0.20)*
Apical HBSS		52	(1.04 ± 0.15)‡	33	(1.07 ± 0.11)‡
Basal HBSS	(−BSA)	12	(0.73 ± 0.25)§	21	(0.73 ± 0.14)§
III Cells		46	(1.43 ± 0.30)*	47	(1.23 ± 0.13)*
Apical HBSS	(−BSA)	34	(0.67 ± 0.13)§	20	(0.66 ± 0.08)§
Basal HBSS		20	(1.22 ± 0.20)‡	32	(1.15 ± 0.27)‡
IV Cells		52	(1.62 ± 0.39)	55	(1.43 ± 0.25)
Apical HBSS	(−BSA)	34	(0.68 ± 0.13)	24	(0.76 ± 0.07)
Basal HBSS	(−BSA)	14	(0.86 ± 0.23)	22	(0.77 ± 0.11)

Cell monolayers were incubated with C6-NBD-ceramide, followed by 2 h at 20°C in the absence of BSA (Materials and Methods). The cells were then incubated for 1 h at 37°C in HBSS containing BSA on both sides (*I*), on the apical side only (*II*), on the basal side only (*III*), or in the absence of BSA (*IV*). 37°C-media without BSA (−BSA) contained no significant fluorescence. The 37°C incubation was followed by 0.5 h at 10°C in HBSS+BSA (twice), after which cells, apical 37- and 10°C-media, and basal media were analyzed. Values (combined 37 and 10°C data) average seven experiments; mean SD, 25%. For (*Test/Control*), within each experiment the data were compared to the control experiment performed with BSA (*I*). Numbers represent average ± SD.

* 1.24 ± 0.23, $n = 28$; a significant increase over control, $p < 0.0005$ in one-tailed t test.

‡ 1.12 ± 0.19, $n = 28$; different from control, $p < 0.005$.

§ 0.70 ± 0.16, $n = 28$; significantly lower than control, $p < 0.0005$.

(14). Independently, the structure labeled by biosynthetic C6-NBD-SPH has been identified as the Golgi complex in a number of cell types; e.g., by the use of authentic Golgi markers (21, 26, 28, 30, 31, 48). C6-NBD-SPH could not be depleted from the Golgi complex by the presentation of a proper acceptor to the cytoplasmic surface in perforated cells (44), providing a direct confirmation of its luminal orientation and the absence of transbilayer flip-flop. Our low temperature results confirm this situation for Caco-2 cells (Table I; Fig. 2). C6-NBD-SPH is synthesized in the Golgi apparatus. Since it does not exchange with other membranes, its orientation must be luminal and transbilayer flip-flop must be absent.

Also most C6-NBD-GlcCer was synthesized intracellularly (Table I). Furthermore, with C6-NBD-GlcCer accounting for 41% of the intracellular fluorescence, we can conclude that also this lipid accumulated in the Golgi complex (Fig. 2 *b*). Indeed, the responsible glucosyltransferase colocalized with the Golgi apparatus rather than plasma membrane (30). The exact location and mechanism of GlcCer biosynthesis remain to be sorted out (6, 46).

The luminal orientation of sphingolipids predicts a vesicular transport mechanism to the cell surface. Indeed, in mitotic cells, where vesicular traffic is inhibited, transport was found to be interrupted for C6-NBD-sphingolipids but not for phosphatidylethanolamine (26), a lipid that can be transported by cytoplasmic exchange (47). Putative Golgi complex–derived carrier vesicles have been isolated from perforated MDCK cells (2). C6-NBD-SPH could not be depleted by BSA, confirming a luminal orientation. In Caco-2, the C6-NBD-lipids remained in the Golgi area below 16°C (Fig. 2), where again vesicular traffic is inhibited (42). At 37°C, they were transported to the plasma membrane, where they became accessible for depletion by BSA (Fig. 4). Alternatively, in the absence of BSA, they were endocytosed (Table IV). Endocytosis and recycling of these lipids displayed characteristics of vesicular transport (27, 28).

In summary, after accumulation in the luminal leaflet of a Golgi cisterna C6-NBD-GlcCer and C6-NBD-SPH are incorporated into budding transport vesicles. After moving across the cytosol, the vesicles fuse to the plasma membrane, whereby their luminal lipids, including the C6-NBD-sphingolipids, are inserted into the topologically equivalent exoplasmic leaflet of the plasma membrane bilayer. From the cell surface, they can be endocytosed and recycled.

Vectorial Transport of Apical C6-NBD-Sphingolipids

C6-NBD-sphingolipids on the one cell surface were not depleted by BSA in the opposite medium, neither at 10°C nor during an hour at 37°C (Tables II and IV). This is in agreement with the presence of a barrier to lipid diffusion between the two surface domains of epithelial cells. The fence has been assigned to the tight junction, and was located in the exoplasmic but not the cytoplasmic leaflet of the plasma membrane bilayer (see references in reference 44). As a consequence, NBD-lipids on the one cell surface could be assayed separately from the NBD-lipids on the opposite surface.

Transport to the cell surface at 37°C was either measured afterwards by a back-exchange at low temperature, or BSA was included in the 37°C incubation media to trap the NBD-lipids upon arrival at the surface (Fig. 3, Table III). If the basolateral surface would be an obligatory stop for apical lipids (see Introduction), at least some of the apical NBD-lipids in transit should be trapped there, resulting in an increased basolateral and decreased apical signal. However, such a reduction in polarity due to the presence of BSA was not observed. Also, there was no evidence for a lag-period

in the transport to the apical surface (Figs. 4 and 5), such as would be expected if lipids before arriving at their final destination first resided temporarily in the opposite domain (and for some reason escaped depletion by the BSA). Neither were the initial apical/basolateral ratios different from those at later time-points. Finally, no substantial transcytosis of NBD-lipids was observed in 1 h (Table IV). Thus, on the time scale of the present experiments, NBD-lipids were transported from the Golgi complex to both surfaces of Caco-2 cells by direct vesicular routes.

Although the membrane surface area transcytosed per hour appears small compared to endocytosis (Table IV), vectorial transcytosis of proteins with half times of hours has been reported in Caco-2 (36). Also for lipids, sorting along the pathway seems necessary to maintain lipid polarity over the lifetime of the cell. To study transcytotic lipid sorting, a more direct assay is needed.

Intracellular Sorting of C6-NBD-Sphingolipids

Since the NBD-lipids were carried to each surface by a direct route only, the polarity of delivery of each lipid must have been determined before its arrival at the cell surface. This polarity was in the order of 2–4 for C6-NBD-GlcCer, but at least twofold lower for C6-NBD-SPH (Tables III, IV; Figs. 3–5), resulting in a relative polarity of 2–3. The C6-NBD-GlcCer/C6-NBD-SPH ratio at the apical surface was, therefore, two- to threefold higher than that at the basolateral surface (Materials and Methods). Since the transport is vesicle mediated, this increased ratio necessarily existed in apical as compared to basolateral vesicles, and, consequently, at the site of apical as compared to basolateral vesicle budding. It has been proposed (45) that such a relative enrichment of C6-NBD-GlcCer over C6-NBD-SPH would be driven by self-aggregation of glycosphingolipids into an apical precursor (micro)domain due to intermolecular hydrogen bonding.

The polarity of delivery of Golgi complex–synthesized C6-NBD-GlcCer and C6-NBD-SPH, especially that in fully differentiated Caco-2 cells (Fig. 1 *b*; Table III), closely reflects the well-characterized equilibrium lipid distribution in intestinal epithelial cells (4, 8, 12, 25). The ratio of the glycosphingolipid concentration in the apical over that in the basolateral plasma membrane, expressed as mole percent of the total lipids, was about 2 (see reference 45), while for the monoglycosyl glycosphingolipids this polarity was 3. In contrast, SPH displayed a polarity of 0.5 (25). The biosynthetic sorting process as characterized by NBD-lipids appears sufficient to generate the in vivo lipid polarity.

Some variation in the apical/basolateral polarity of specific glycosphingolipids has been observed in enterocytes (17). For bulk glycosphingolipids, the monoglycosyl species and the complex globoside, the polarity was 3–5. Gangliosides were not polarized (25). The variation may be a consequence of differences in the intermolecular interaction energy, which in fact is highest for the simple glycolipid GlcCer (34).

The relative polarity of C6-NBD-GlcCer as compared to C6-NBD-SPH in the human intestinal cell line Caco-2 was very similar to that found in the dog kidney–derived MDCK cells (cf., Table III with reference 48). This predicts a general, conserved mechanism for epithelial plasma membrane lipid sorting (47). In contrast, the sorting of plasma membrane proteins in Caco-2 cells appears less stringent than that in MDCK cells (32, 36). At first sight, this seems in conflict with the idea that the sorting of lipids and that of proteins are closely interlinked. However, it should be realized that, so far, for no single membrane protein has sorting been compared between both cell types. In addition, even if the protein sorting is really different, the sorting principle may be identical. Incomplete sorting in the *trans*-Golgi network of Caco-2 cells might be a consequence of a reduced capacity of the sorting machinery. The latter might be due to the limiting amount of a single component; e.g., the putative sorter protein (45). Alternatively, it might be a consequence of the reduced size of the apical pathway in Caco-2 cells that has been suggested by others (23, 36, 40). Our present findings provide no support for such a minor apical pathway in Caco-2 cells. The apical/basolateral ratio of lipid transport from the Golgi apparatus to the plasma membrane for both C6-NBD-GlcCer and C6-NBD-SPH was identical to that in MDCK, where the occurrence of substantial membrane flow from Golgi complex to both the apical and basolateral surface is generally accepted. It is therefore important to establish true nonspecific markers for the measurement of the relative apical and basolateral pathway sizes. An understanding of the factors by which these relative sizes are determined probably has to await the elucidation of the preceding sorting process, a major challenge in epithelial cell biology.

We are grateful to Judith Klumperman and Hans-Peter Hauri (Biocenter, University of Basel, Switzerland) for the Caco-2 cells and helpful suggestions. We thank Willem Hage (Hubrecht Laboratory) for providing the confocal images in Fig. 2, Tineke Veenendaal for her part in the electron-microscopy, René Scriwanek for expert darkroom assistance, and Henry Laning for fine experimental contributions. The Transwell-COL filters were kindly donated by Hank Lane (Costar). We are grateful to Dirk Cerneus, Ida van Genderen, and Alex Sandra (University of Iowa) for critically reading the manuscript.

The present work was made possible by a senior fellowship from the Royal Netherlands Academy of Arts and Sciences to G. van Meer.

Received for publication 13 March 1990 and in revised form 17 May 1990.

References

1. Ahnen, D. J., N. A. Santiago, J.-P. Cezard, and G. M. Gray. 1982. Intestinal aminooligopeptidase. In vivo synthesis on intracellular membranes of rat jejunum. *J. Biol. Chem.* 257:12129–12135.
2. Bennett, M. K., A. Wandinger-Ness, and K. Simons. 1988. Release of putative exocytic transport vesicles from perforated MDCK cells. *EMBO (Eur. Mol. Biol. Organ.) J.* 7:4075–4085.
3. Bligh, E. G., and W. J. Dyer. 1959. A rapid method of total lipid extraction and purification. *Can. J. Biochem. Physiol.* 37:911–917.
4. Brasitus, T. A., and D. Schachter. 1980. Lipid dynamics and lipid-protein interactions in the rat enterocyte basolateral and microvillus membranes. *Biochemistry.* 19:2763–2769.
5. Caplan, M., and K. S. Matlin. 1989. Sorting of membrane and secretory proteins in polarized epithelial cells. *In* Modern Cell Biology. B. H. Satir, editor. Functional Epithelial Cells in Culture. K. S. Matlin, J. D. Valentich, editors. Alan R. Liss, Inc., New York. 71–127.
6. Coste, H., M. B. Martel, and R. Got. 1986. Topology of glucosylceramide synthesis in Golgi membranes from porcine submaxillary glands. *Biochim. Biophys. Acta.* 858:6–12.
7. Danielsen, E. M., and G. M. Cowell. 1985. Biosynthesis of intestinal microvillar proteins. Evidence for an intracellular sorting taking place in, or shortly after, exit from the Golgi complex. *Eur. J. Biochem.* 152:493–499.
8. Douglas, A. P., R. Kerley, and K. J. Isselbacher. 1972. Preparation and characterization of the lateral and basal plasma membranes of the rat intestinal epithelial cell. *Biochem. J.* 128:1329–1338.
9. Eilers, U., J. Klumperman, and H.-P. Hauri. 1989. Nocodazole, a microtubule-active drug, interferes with apical protein delivery in cultured intestinal epithelial cells (Caco-2). *J. Cell Biol.* 108:13–22.
10. Faust, R. A., and J. J. Albers. 1988. Regulated vectorial secretion of cho-

lesteryl ester transfer protein (LTP-I) by the CaCo-2 model of human enterocyte epithelium. *J. Biol. Chem.* 263:8786–8789.
11. Field, F. J., E. Albright, and S. N. Mathur. 1988. Regulation of triglyceride-rich lipoprotein secretion by fatty acids in CaCo-2 cells. *J. Lipid Res.* 29:1427–1437.
12. Forstner, G. G., K. Tanaka, and K. J. Isselbacher. 1968. Lipid composition of the isolated rat intestinal microvillus membrane. *Biochem. J.* 109: 51–59.
13. Fransen, J. A. M., L. A. Ginsel, H.-P. Hauri, E. Sterchi, and J. Blok. 1985. Immunoelectronmicroscopical localization of a microvillus membrane disaccharidase in the human small intestinal epithelium with monoclonal antibodies. *Eur. J. Cell Biol.* 38:6–15.
14. Futerman, A. H., B. Stieger, A. L. Hubbard, and R. E. Pagano. 1990. Sphingomyelin synthesis in rat liver occurs predominantly at the cis and medial cisternae of the Golgi apparatus. *J. Biol. Chem.* 265:8650–8657.
15. Grasset, E., M. Pinto, E. Dussaulx, A. Zweibaum, and J.-F. Desjeux. 1984. Epithelial properties of human colonic carcinoma cell line Caco-2: electrical parameters. *Am. J. Physiol.* 247:C260–C267.
16. Hansen, G. H., H. Sjöström, O. Norén, and E. Dabelsteen. 1987. Immunomicroscopic localization of aminopeptidase N in the pig enterocyte. Implications for the route of intracellular transport. *Eur. J. Cell Biol.* 43: 253–259.
17. Hansson, G. C. 1983. The subcellular localization of the glycosphingolipids in the epithelial cells of rat small intestine. *Biochim. Biophys. Acta.* 733:295–299.
18. Hauri, H.-P., A. Quaroni, and K. J. Isselbacher. 1979. Biogenesis of intestinal plasma membrane: posttranslational route and cleavage of sucrase-isomaltase. *Proc. Natl. Acad. Sci. USA.* 76:5183–5186.
19. Hauri, H.-P., E. E. Sterchi, D. Bienz, J. A. M. Fransen, and A. Marxer. 1985. Expression and intracellular transport of microvillus membrane hydrolases in human intestinal epithelial cells. *J. Cell Biol.* 101:838–851.
20. Hidalgo, I. J., T. J. Raub, and R. T. Borchardt. 1989. Characterization of the human colon carcinoma cell line (Caco-2) as a model system for intestinal epithelial permeability. *Gastroenterology.* 96:736–749.
21. Ho, W. C., V. J. Allan, G. van Meer, E. G. Berger, and T. E. Kreis. 1989. Reclustering of scattered Golgi elements occurs along microtubules. *Eur. J. Cell Biol.* 48:250–263.
22. Hubbard, A. L., B. Stieger, and J. R. Bartles. 1989. Biogenesis of endogenous plasma membrane proteins in epithelial cells. *Annu. Rev. Physiol.* 51:755–770.
23. Hughson, E. J., D. F. Cutler, and C. R. Hopkins. 1989. Basolateral secretion of kappa light chain in the polarised epithelial cell line, Caco-2. *J. Cell Sci.* 94:327–332.
24. Jeckel, D., A. Karrenbauer, R. Birk, R. R. Schmidt, and F. Wieland. 1990. Sphingomyelin is synthesized in the cis-Golgi. *FEBS (Fed. Eur. Biochem. Soc.) Lett.* 261:155–157.
25. Kawai, K., M. Fujita, and M. Nakao. 1974. Lipid components of two different regions of an intestinal epithelial cell membrane of mouse. *Biochim. Biophys. Acta.* 369:222–233.
26. Kobayashi, T., and R. E. Pagano. 1989. Lipid transport during mitosis. Alternative pathways for delivery of newly synthesized lipids to the cell surface. *J. Biol. Chem.* 264:5966–5973.
27. Kok, J. W., S. Eskelinen, K. Hoekstra, and D. Hoekstra. 1989. Salvage of glucosylceramide by recycling after internalization along the pathway of receptor-mediated endocytosis. *Proc. Natl. Acad. Sci. USA.* 86:9896–9900.
28. Koval, M., and R. E. Pagano. 1989. Lipid recycling between the plasma membrane and intracellular compartments: transport and metabolism of fluorescent sphingomyelin analogues in cultured fibroblasts. *J. Cell Biol.* 108:2169–2181.
29. Le Bivic, A., F. X. Real, and E. Rodriguez-Boulan. 1989. Vectorial targeting of apical and basolateral plasma membrane proteins in a human adenocarcinoma epithelial cell line. *Proc. Natl. Acad. Sci. USA.* 86:9313–9317.
30. Lipsky, N. G., and R. E. Pagano. 1985*a*. Intracellular translocation of fluorescent sphingolipids in cultured fibroblasts: endogenously synthesized sphingomyelin and glucocerebroside analogues pass through the Golgi apparatus en route to the plasma membrane. *J. Cell Biol.* 100: 27–34.
31. Lipsky, N. G., and R. E. Pagano. 1985*b*. A vital stain for the Golgi apparatus. *Science (Wash. DC).* 228:745–747.
32. Lisanti, M. P., A. Le Bivic, M. Sargiacomo, and E. Rodriguez-Boulan. 1989. Steady-state distribution and biogenesis of endogenous Madin-Darby canine kidney glycoproteins: evidence for intracellular sorting and polarized cell surface delivery. *J. Cell Biol.* 109:2117–2127.
33. Lorenzsonn, V., H. Korsmo, and W. A. Olsen. 1987. Localization of sucrase-isomaltase in the rat enterocyte. *Gastroenterology.* 92:98–105.
34. Maggio, B., F. A. Cumar, and R. Caputto. 1978. Surface behaviour of gangliosides and related glycosphingolipids. *Biochem. J.* 171:559–565.
35. Massey, D., H. Feracci, J.-P. Gorvel, A. Rigal, J. M. Soulié, and S. Maroux. 1987. Evidence for the transit of aminopeptidase N through the basolateral membrane before it reaches the brush border of enterocytes. *J. Membr. Biol.* 96:19–25.
36. Matter, K., M. Brauchbar, K. Bucher, and H.-P. Hauri. 1990. Sorting of endogenous plasma membrane proteins occurs from two sites in cultured human intestinal epithelial cells (Caco-2). *Cell.* 60:429–437.
37. Neutra, M., and D. Louvard. 1989. Differentiation of intestinal cells in vitro. *In* Modern Cell Biology. B. H. Satir, editor. K. S. Matlin and J. D. Valentich, editors. Alan R. Liss, Inc., New York. 363–398.
38. Pinto, M., S. Robine-Leon, M.-D. Appay, M. Kedinger, N. Triadou, E. Dussaulx, B. Lacroix, P. Simon-Assmann, K. Haffen, J. Fogh, and A. Zweibaum. 1983. Enterocyte-like differentiation and polarization of the human colon carcinoma cell line Caco-2 in culture. *Biol. Cell.* 47: 323–330.
39. Quaroni, A., K. Kirsch, and M. M. Weiser. 1979. Synthesis of membrane glycoproteins in rat small-intestinal villus cells. Redistribution of L-[1,5, 6-^{3}H]fucose-labeled membrane glycoproteins among Golgi, lateral basal and microvillus membranes in vivo. *Biochem. J.* 182:203–212.
40. Rindler, M. J., and M. G. Traber. 1988. A specific sorting signal is not required for the polarized secretion of newly synthesized proteins from cultured intestinal epithelial cells. *J. Cell Biol.* 107:471–479.
41. Rodriguez-Boulan, E., and W. J. Nelson. 1989. Morphogenesis of the polarized epithelial cell phenotype. *Science (Wash. DC).* 245:718–725.
42. Saraste, J., G. E. Palade, and M. G. Farquhar. 1986. Temperature-sensitive steps in the transport of secretory proteins through the Golgi complex in exocrine pancreatic cells. *Proc. Natl. Acad. Sci. USA.* 83:6425–6429.
43. Simons, K., and S. D. Fuller. 1985. Cell surface polarity in epithelia. *Annu. Rev. Cell Biol.* 1:243–288.
44. Simons, K., and H. Virta. 1987. Perforated MDCK cells support intracellular transport. *EMBO (Eur. Mol. Biol. Organ.) J.* 6:2241–2247.
45. Simons, K., and G. van Meer. 1988. Lipid sorting in epithelial cells. *Biochemistry.* 27:6197–6202.
46. Suzuki, Y., C. P. Ecker, and H. A. Blough. 1984. Enzymatic glucosylation of dolichol monophosphate and transfer of glucose from isolated dolichyl-D-glucosyl phosphate to ceramides by BHK-21 cell microsomes. *Eur. J. Biochem.* 143:447–453.
47. van Meer, G. 1989. Lipid traffic in animal cells. *Annu. Rev. Cell Biol.* 5:247–275.
48. van Meer, G., E. H. K. Stelzer, R. W. Wijnaendts-van-Resandt, and K. Simons. 1987. Sorting of sphingolipids in epithelial (Madin-Darby canine kidney) cells. *J. Cell Biol.* 105:1623–1635.